Carbohydrate Polymers 99 (2014) 74–83

Contents lists available at ScienceDirect

Carbohydrate Polymers

journal homepage: www.elsevier.com/locate/carbpol

Control of size and viscoelastic properties of nanofibrillated cellulose from palm tree by varying the TEMPO-mediated oxidation time

Karima Benhamou[a,b], Alain Dufresne[b], Albert Magnin[c], Gérard Mortha[b], Hamid Kaddami[a,*]

[a] Cadi Ayyad University, Faculty of Sciences and Technologies, Laboratory of Organometallic and Macromolecular Chemistry, Avenue Abdelkrim Elkhattabi, B.P. 549, Marrakech, Morocco
[b] The International School of Paper, Print Media and Biomaterials (Pagora), Grenoble Institute of Technology, CS10065, 38402 Saint Martin d'Héres, France
[c] Laboratoire Rhéologie et Procédés, Grenoble-INP, UJF Grenoble 1, UMR CNRS 5520, BP 53, 38041 Grenoble Cedex 9, France

ARTICLE INFO

Article history:
Received 14 February 2013
Received in revised form 6 August 2013
Accepted 15 August 2013
Available online 20 August 2013

Keywords:
TEMPO-mediated oxidation
Nanofibrillated cellulose (NFC)
Oxidation time
Date palm tree
Zeta-potential
Viscoelastic properties

ABSTRACT

The main objective of the present study was to control and optimize the preparation of nanofibrillated cellulose (NFC) from the date palm tree by monitoring the oxidation time (degree of oxidation) of the pristine cellulose and the number of cycles through the homogenizer. The oxidation was monitored by TEMPO (1-oxo-2,2,6,6-tétraméthylpipyridine 1-oxyle) mediated oxidation. Evidence of the successful isolation of NFC was given by FE-SEM observation revealing fibrils with a width in the range 20–30 nm, depending of the oxidation time. The evolution of the transparency of the aqueous NFC suspension and carboxylic content according to the degree of oxidation and number of cycles were also analyzed by UV–vis transmittance, Fourier-transform infrared spectroscopy (FT-IR), conductimetry, and X-ray diffraction analysis. A significant NFC length reduction occurred during the TEMPO-mediated oxidation.

The rheological properties of NFC suspensions were characterized as function of the oxidation time. Dynamic rheology showed that the aqueous suspension behavior changed from liquid to gel depending on the concentration. The highest concentration studied was 1 wt% and the modulus reached 1 MPa which was higher than for non-oxidized NFC. An explanation of the gel structure evolution with the oxidation time applied to the NFC (NFC length) was proposed. The gel structure evolves from an entanglement-governed gel structure to an immobilized water molecule-governed one.

1. Introduction

Cellulose microfibrils extracted from the wood cell wall offer a potential for designing new materials with new properties. This is because components with nanoscale dimensions have different properties from those of their bulk counterparts. Nanofibrillated cellulose (NFC) disintegrated from wood pulp has high length-to-width ratio, high stiffness and ability to form networks through strong secondary bonding, including hydrogen bonds. This allows significant design freedom for the development of new materials. From highly porous foams to reinforced polymer composites and dense nanopaper structures, the utilization possibilities are promising. There are many potential applications, including kinetic energy absorbers, packaging, thermal and acoustic insulating materials, substrates for electronic displays, reinforcement networks and scaffolds for nanocomposites, pharmaceutical and biomedical applications (i.e. drug carriers, tissue engineering scaffolds), and as storage materials with high specific surface area. However, good control of the nanostructure of the fibrils is crucial in order to achieve the desired properties. Such a control of the structure requires deeper understanding on how the processing affects the material structure.

NFC consists of cellulose microfibril aggregates that have been disintegrated from the cellulosic substrate. The first disintegration process dates back to the 1980s when Turbak et al. subjected a wood pulp suspension to high shear forces by passing it several times through a homogenizer (Turbak, Snyder, & Sandberg, 1983). During this process, the reciprocating action of the valve, coupled with the large pressure drop and impact with the valve seat resulted in cellulose fibrillation, and a thick aqueous dispersion of cellulose fibrils with a diameter of 25–100 nm was produced. The initial terminology used by Turbak et al. (1983) was microfibrillated cellulose (MFC), and this is still in use although it may confuse the reader since the lateral dimension of the fibrils is far below the micrometer scale.

The most affordable disintegration procedure giving 3–5 nm NFC has however be demonstrated by Saito et al., where chemically pretreated pulp (by TEMPO-mediated oxidation) can be

* Corresponding author. Tel.: +212 0661071386; fax: +212 0524433170.
E-mail addresses: h.kaddami@uca.ma, hkaddami@yahoo.fr (H. Kaddami).

0144-8617/$ – see front matter © 2013 Elsevier Ltd. All rights reserved.
http://dx.doi.org/10.1016/j.carbpol.2013.08.032

disintegrated by a kitchen blender or even using magnetic stirring (Saito, Kimura, Nishiyama, & Isogai, 2007). TEMPO-mediated oxidation is expected to result in improved NFC individualization by electrostatic repulsion from the introduction of negatively charged surface groups (Montanari, Roumani, Heux, & Vignon, 2005). Acid hydrolysis, alkaline, and enzymatic hydrolysis are commonly used in the wood and paper industry. However, TEMPO is an emerging technology not commonly used in industrial applications related to the pulp and paper industries. A major challenge for the industrial application of TEMPO is cost, but a significant energy reduction in producing NFC could overcome this drawback and promote the production of this renewable material for new applications. Advantages of using TEMPO oxidation for polysaccharides, in comparison to acid, are high reaction rate, yield, and selectivity while only minimal degradation (Bragd, van Bekkum, & Besmer, 2004). Reaction time for the common pretreatments may cause issues for industrial scale up, but the reaction rate for TEMPO can be monitored with temperature, TEMPO concentration, and NaBr concentration, temperature being the most significant parameter (Suh, Lee, Chang, & Kim, 2007). It is believed that TEMPO assists in producing NFC by loosening adhesion between the microfibrils and introducing electrostatic repulsion between them (Saito, Nishiyama, Putaux, Vignon, & Isogai, 2006). The extent of pulp fiber disintegration depends not only on the mechanical device used but also on parameters such as:

- The number of passes through the mechanical device: a higher number of passes leads to more efficient disintegration. However, above a certain number, degradation of the fibrils starts (e.g. kinks) and this lowers the quality of NFC.
- The pretreatment of the pulp fiber: subjecting the pulp fiber to a pretreatment prior to mechanical disintegration considerably facilitates the disintegration process and lowers the number of passes required through the mechanical device. Examples of pretreatments include enzymatic hydrolysis (Henriksson, Henriksson, Berglund, & Lindstrom, 2007; Pääkkö et al., 2007) and oxidation of the cellulose fibril surface (Saito et al., 2007).

The number of papers in literature dealing with the control of NFC length is very low. While studying the relationship between the plant characteristics and the NFC extraction, Alila, Besbes, Rei Vilar, Mutjé, and Boufi (2013) showed that the length of NFC depends on the cellulose origin. Shinoda, Saito, Okita, and Isogai (2012) studied the effect of the degree of oxidation on the NFC length. Both Alila et al. and Shinoda et al. used viscosimetric measurement to estimate the NFC length. Ishii, Saito, and Isogai (2011) used viscoelastic measurements to estimate the NFC length.

In our study, we successfully prepared NFC dispersions extracted from date palm tree using TEMPO-mediated oxidation while acting on the degree of oxidation and the number of cycles through the homogenizer. Several experimental techniques have been used in this study to characterize the produced NFC such FE-SEM, UV–vis and FT-IR spectroscopies, conductimetry, and X-ray diffraction analysis. The aim was to evaluate the effect of oxidation time on the NFC aspect ratio in the TEMPO-mediated reaction conditions usually used in our laboratory (Sbiai, Kaddami, Sautereau, Maazouz, & Fleury, 2011). The main difference between our approach and the one reported by Shinoda et al. (2012) lies on how to change the degree of oxidation of NFC. Actually, it is based on the work we carried out showing that the reaction kinetics of TEMPO-mediated oxidation can be controlled by choosing the appropriate reaction conditions (temperature and concentration of reactants). The aim here was to see if by changing the degree of oxidation we can have the same effect on the NFC size.

Another scope of the present paper is to conduct a comprehensive study of the rheological measurements of oxidized microfibrils solutions and gels in water, and to study the effect of the oxidation degree on the rheological behavior of its suspensions.

2. Experimental

2.1. Materials

The rachis of date palm tree (*Phoenix dactylifera L.*) was used in this work as the original source of cellulose. Cellulose was extracted from the rachis following the procedure well described in our previous work (Bendahou, Habibi, Kaddami, & Dufresne, 2009). TEMPO, sodium bromide, sodium hypochlorite solution (15%), HCl, and NaOH were purchased from Sigma–Aldrich and used without further purification.

2.2. Pretreatment procedure

The general procedure and reagent ratios used by Sbiai et al. (2011) were used for TEMPO-mediated oxidation of cellulose fibers. About 2 g, i.e. 2.136 mmol of equivalent anydroglucose unit (AGU) of cellulose, were suspended in water (200 ml) and sonicated with a Branson Sonifier for 5 min. TEMPO (32 mg, 0.065 mmol) and NaBr (0.636 g, 1.9 mmol) were added to the suspension. A certain amount of the NaOCl solution, corresponding to 40.5 ml was added drop wise to the cellulose suspension. The pH was adjusted at 10 by addition of a 0.1 M aqueous solution of HCl. The pH of the mixture was maintained to 10 at 4 °C by continuous adding of 0.1 M NaOH while stirring the suspension. After times ranging from 5 to 120 min, the oxidation was terminated by adding methanol (5 ml) and the pH was adjusted to 7 by adding 0.1 M HCl.

Various samples differing by the oxidation time were prepared. The oxidation times chosen were: 5 min, 15 min, 30 min, 1 h and 2h.

2.3. Homogenization

After pretreatment, a 2% fiber suspension in water was subjected to the homogenizing action of low-pressure slit homogenizer using Laboratory Homogenizer PANDA 2K (GEA Niro Soavi S.p.A), USA. Oxidized cellulose was disintegrated by pumping the suspension up to 15 times through the homogenizer. Efforts were made to keep the pressure constant at 650 MPa for all cycles and all samples. During the process, the viscosity and the temperature of the suspension increased with increasing the number of passes. The maximum temperature reached was 70 °C. Herrick, Casebier, Hamilton, and Sandberg (1983) found that increasing the temperature from 20 °C to 70–80 °C facilitated the homogenization process.

3. Characterization

3.1. Surface chemical properties – FTIR

Effect of the pretreatment on surface chemistry of NFC was examined by FTIR. Infrared spectra were recorded on a FT-IR Perkin-Elmer 1000 spectrometer collecting 32 scans from 400 to 4000 cm^{-1}. Transmission FTIR was performed on NFC films prepared by heat-drying NFC suspensions. A separate background spectrum was collected and automatically subtracted from the raw spectrum for each specimen.

3.2. Carboxyl content on oxidized NFC – conductimetric titration (CT)

The carboxyl content of oxidized cellulose samples was determined by conductimetric titration. The cellulose samples (45.5 mg)

were suspended into 15 ml of 0.01 M hydrochloric acid solutions. After 30 min stirring, the suspension was titrated with 0.01 M NaOH. The titration curves showed the presence of a strong acid (V_1) corresponding to the excess of HCl and a weak acid (V_2) corresponding to the carboxyl content. The carboxylic content was given by:

$$n(\text{COOH}) = 0.01 \times (V_2 - V_1) \times 0.01 \quad (1)$$

3.3. Yield of fibrillation

A diluted suspension (0.2% solid content) was centrifuged at 5000 rpm for 30 min to separate the nanofibrillated material (in supernatant fraction) from unfibrillated and partially fibrillated fibers which sedimented. The sediment fraction was dried to constant weight at 90 °C in a halogen desiccator and the yield of the nanofibrillated fraction was calculated from:

$$\text{Yield\%} = \left[1 - \frac{\text{weight of dried sediment}}{(\text{weight of dried sediment}) \times \%Sc}\right] \times 100 \quad (2)$$

Where Sc%, solid content of the diluted dispersion sample.

3.4. Carbohydrate composition – (HPLC)

High performance liquid chromatography (HPLC) has been used to characterize the carbohydrate composition of the pristine cellulose according to Tappi rules TAPPI T249 OM-85.

3.5. Crystallinity index – X-ray diffraction (XRD) analysis

NFC Films were prepared by heat-drying method and were examined using XRD to evaluate the impact of the treatment on the crystallinity index of NFC. Bleached cellulose film was prepared and used as reference.

A XPERT-MPD wide angle X-ray diffractometer operated at 40 kv and 30 mA with a Ni-filtered CuKα radiation was used to determine the crystallinity index of the specimens. X-ray diffractograms were recorded at 0.02° s^{-1} over a 2θ scan in the range 10–60°. Crystallinity index (C.I.) values were calculated according to the empirical Segal method (Segal, Creely, Martin, & Conrad, 1959):

$$\text{C.I.} = \frac{I_{002} - I_{AM}}{I_{002}} \times 100 \quad (3)$$

Where I_{002} is the intensity of the 002 reflection (2θ between 22° and 23°) and I_{AM} is the minimum value at 2θ between 18° and 19°, which represents the reflection intensity of the amorphous phase.

3.6. Estimation of the degree of polymerization of cellulose

The degree of polymerization of cellulose chains forming NFC can be estimated from the average intrinsic viscosity value. For cellulose, the intrinsic viscosity, [η] (dl/g), is related to the degree of polymerization (DP) and empirical relationship for this polymer-solvent system is suggested as (Rinaudo, 1968):

$$[\eta] = 0.891\, DP^{0.936} \quad (4)$$

The measurements were performed for dissolved NFC in cuprietylendiamine (1 N) as solvent. For each NFC sample, three different concentrations were prepared to determine the intrinsic viscosity. For each concentration, the efflux time was averaged on three measurements at 25 ± 0.1 °C. The intrinsic viscosity of bleached cellulose was calculated to serve as reference.

3.7. Microscopy – field emission scanning electron microscopy (FE-SEM)

The model quanta 200FEI, with accelerating voltage of 12.5 kV was used. A drop of the NFC suspension, with a very low solid content of about 10^{-5}%, was deposited on a carbon-coated grid and coated with a thin layer of gold.

3.8. Optical transmittance

NFC water suspension was introduced into a quartz cuvette, and the transmittance was measured from 325 to 800 nm using a "Cecil, CE1010 UV"-vis spectrometer. The spectrum of a cuvette filled with distilled water was used as reference.

3.9. Zeta potential measurements

Zeta potential measurements were carried using the zeta-meter "Zetasizer DTS0230 Malvern Instruments". The ionic strength of the dispersion medium was the same for all measurements and was stabilized at 0.01 M using NaCl solution.

3.10. Dynamic rheology

The rheological measurements were carried out using a controlled stress instrument (ARES G2 TA Rheometer, France) equipped with acrylic parallel-plate (d = 50 mm) geometry at controlled temperature 23 ± 0.1 °C, and the gap used was 1 mm. Covers around samples were used to avoid water evaporation during measurements. Before each measurement, the samples were allowed to rest for 5–10 min.

The oscillation strain amplitude sweep studies were conducted at a frequency of 1 Hz over the range of 1–100% (log–log mode). The resulting viscoelastic parameters were monitored.

The frequency sweep was carried in the range of 0.1–100 Hz at a controlled strain of 5% strain (linear viscoelastic region).

4. Results and discussion

4.1. NFC preparation and characterization

The characteristics of the samples obtained for various oxidation times are listed in Table 1. No NFC could be obtained when subjecting unoxidized cellulose (sample 1 – Table 1) to 15 mechanical shearing passes at 650 MPa On the other hand, the carboxylate content increases with reaction time and consequently the provided carboxylic groups throughout the surface of the microfibrils within the fibers generate repulsive forces that favor the breakdown of the cohesion among the microfibrils held by hydrogen bonding.

FTIR measurements were performed to confirm qualitatively the level of oxidation achieved on the oxidized NFC. Fig. 1 shows the FTIR spectra for pristine cellulose (sample 1 – Table 1) and oxidized NFC (samples 2–6) – Table 1. In these figures, the circled area near 1730 cm^{-1} corresponds to the C=O stretching frequency of carboxyl groups in their acidic form. It is worth noting the absence of the 1730 cm^{-1} band for pristine cellulose, as expected since the content of carboxylic group in the pristine cellulose was too small. As NFC was oxidized a peak at 1730 cm^{-1} is observed and the magnitude of this peak increases as the oxidation time increased.

The yield values are high indicating that almost all bleached cellulose was disintegrated after 15 cycles regardless the oxidation time. When the carboxylic content reached 260 μmol/g only three passes through the homogenizer were sufficient to yield 100% of defibrillation. This result indicates that the reaction occurred rather homogeneously throughout the fiber and that the disintegration did not require the complete oxidation of the surface.

Table 1
Characteristics of the pristine date palm tree cellulose and TEMPO-oxidized cellulose samples.

Sample	Reaction time [min]	COONa content [μmol/g]	Estimated DP	Nb of cycles through the homogenizer	Yield %	Crystallinity index (%)	Zeta potential ζ(mV) at pH = 5
1	0	177	650	0	–	72	–
				3	0	–	
				6	0	–	
				9	0		
				12	0		
				15	0		
	5	221	500	0	–	72	−40.4 ± 1.3
2				3	82	71.6	
				6	92	68.6	
				9	94.5	66.1	
				12	97.3	65.7	
				15	99.3	62.2	
3	15	265	390	0	–	72	−44.9 ± 0.7
				3	85	–	
				6	93.1	–	
				9	96.5	–	
				12	99.1	–	
				15	99.8	–	
4	30	442	215	0	–	72	−50.8 ± 2.2
				3	100	–	
5	60	575	130	0	–	72	−53.5 ± 1.5
				3	100	–	
6	120	774	100	0	–	72	−59.1 ± 3.7
				3	100	70	
				6		69.3	
				9		67.7	
				12		–	
				15		58.1	

The easy disintegration of NFC from the rachis of date palm tree could be explained by the high content of hemicelluloses existing in the bleached cellulose that might facilitate the release of the fibrils (see supporting data (S1)). The relatively low crystallinity index of pristine cellulose is another parameter that might facilitate the disintegration process (Alila et al., 2013).

Supplementary data related to this article found, in the online version, at http://dx.doi.org/10.1016/j.carbpol.2013.08.032.

UV–vis spectroscopy was performed on NFC to get preliminary information on the effect of the studied experimental parameters on the NFC size. The UV–vis transmittance analyses for NFC dispersion samples 2, 4 and 6 are presented in Fig. 2A–C, respectively. The transmittance was measured as a function of reaction time and number of passes through the homogenizer. The transmittance is wavelength-dependent and it decreases for decreasing wavelengths, as light scatters more when the wavelength approaches the diameter of the particles. For suspended fibrils or rods thinner than the wavelength, the light scattering is proportional to the mass/length ratio or the cross section area.

The photographs presented in Fig. 2A–C show the appearance of the 0.1% NFC suspensions with different oxidation times and numbers of passes through the homogenizer. For all samples, a transparent dispersion was obtained after 3 passes. The fairly higher transparency degree was observed for samples presenting the highest degree of oxidation (2 h), namely for the sample with carboxylic content 774 μmol/g.

Further evidence of the effect of the preparation conditions on the transparency of the NFC suspensions is depicted from UV–vis

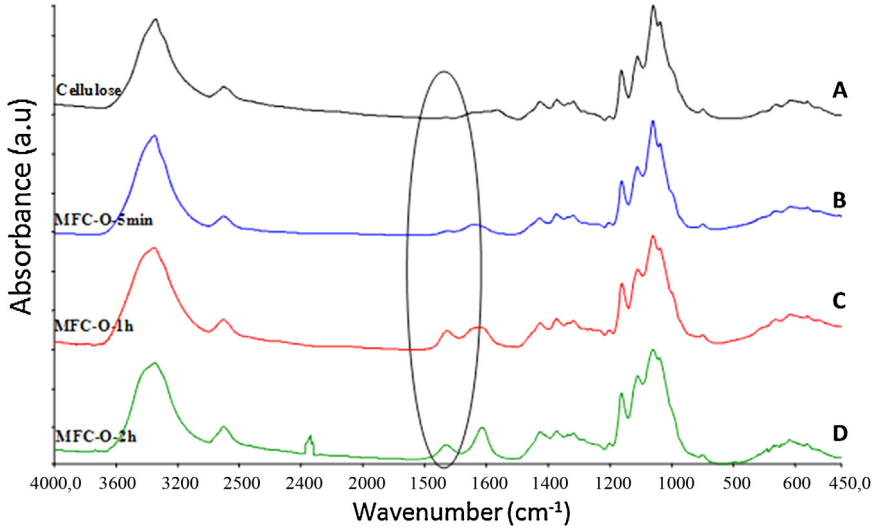

Fig. 1. FT-IR spectra of pristine cellulose and NFC: (A) pristine cellulose (sample 1) and cellulose oxidized for different times: (B) sample 3 (15 min oxidation), (C) sample 5 (1 h oxidation), and (D) sample 6 (2 h oxidation).

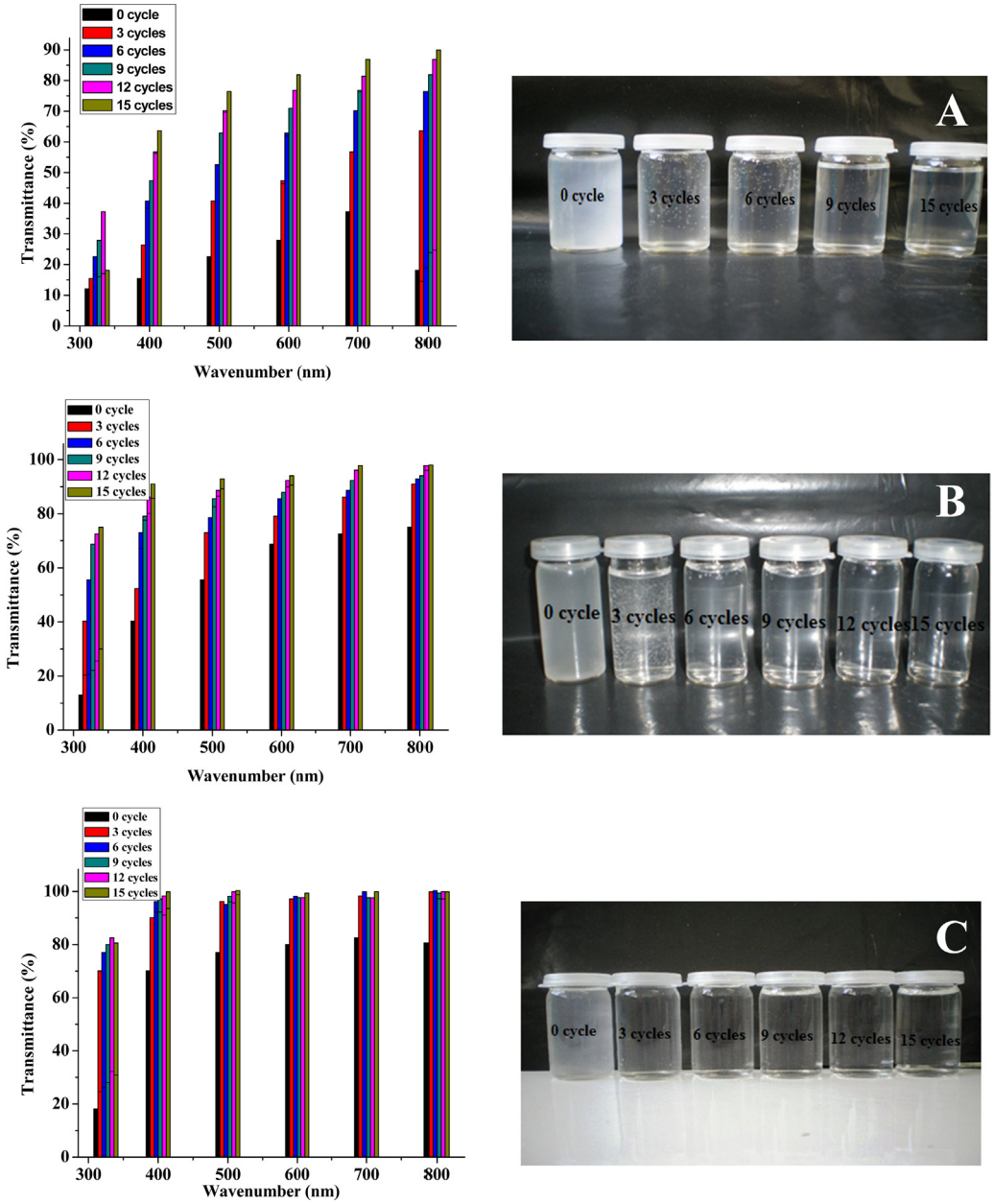

Fig. 2. UV–visspectroscopy and visual appearance of the NFC suspensions as a function of thenumber of passes through the homogenizer; (A) NFC-5 minoxidation, (B) NFC-30 min oxidation, (C) NFC-120 min oxidation.

transmittance spectra of diluted suspension (Fig. 2A–C). One can see from these results that the disintegration proceeds as much as the number of passes through the homogenizer is increased. On the other hand it is clear that the transmittance is higher for sample 6 suspensions (Fig. 2C) followed by those of sample 3 (Fig. 2B), while sample 2 dispersion (Fig. 2A) shows the lowest transmittance (see characteristics for these samples in Table 1). This could be explained by the reduction of the fibril size as the oxidation time, or the carboxyl groups content on the fibril surface, is increased.

The measurement of the degree of polymerization (DP) confirms the reduction of NFC size when the oxidation time increased. However, it is worth noting that this measurement has been achieved by viscosimetric method by mean of equation (3) using the exponent $a = 0.891$ and $K = 0.936$ typically used for cellulose, resulting in incorrect value of the degree of polymerization. Nevertheless, this enables to have a true qualitative idea of the evolution of the degree of polymerization with oxidation time. The results are presented in Table 1 and it shows that although the TEMPO-mediated oxidation of the fibers was carried out at low temperature to avoid the depolymerization through β-elimination of glycoside bonds (Saito et al., 2009), a drastic drop of DP occurred. This phenomenon is expected to be the result of the cleavage of the (1–4)-β-glycoside bonds by hydroxyl and/or other active radical species formed in situ, as side reactions during TEMPO-mediated oxidation (Shibata, Yanagisawa, Sato, & Isogai, 2006).

The morphology of NFC and pristine cellulose was characterized by FE-SEM (Fig. 3). The fibers in the pristine cellulose sample were about 30 μm wide and some hundred of micrometers long (Fig. 3a). The micrograph of NFC extracted after 5 min TEMPO-mediated oxidation is presented in Fig. 6b and one can distinguish fibrils of more than 2 μm long and about 40 nm wide. These fibrils show high aspect ratio and are comparable to those obtained by high mechanical shearing using microfluidizer without any oxidative pretreatment (Bendahou, Kaddami, & Dufresne, 2010). When the

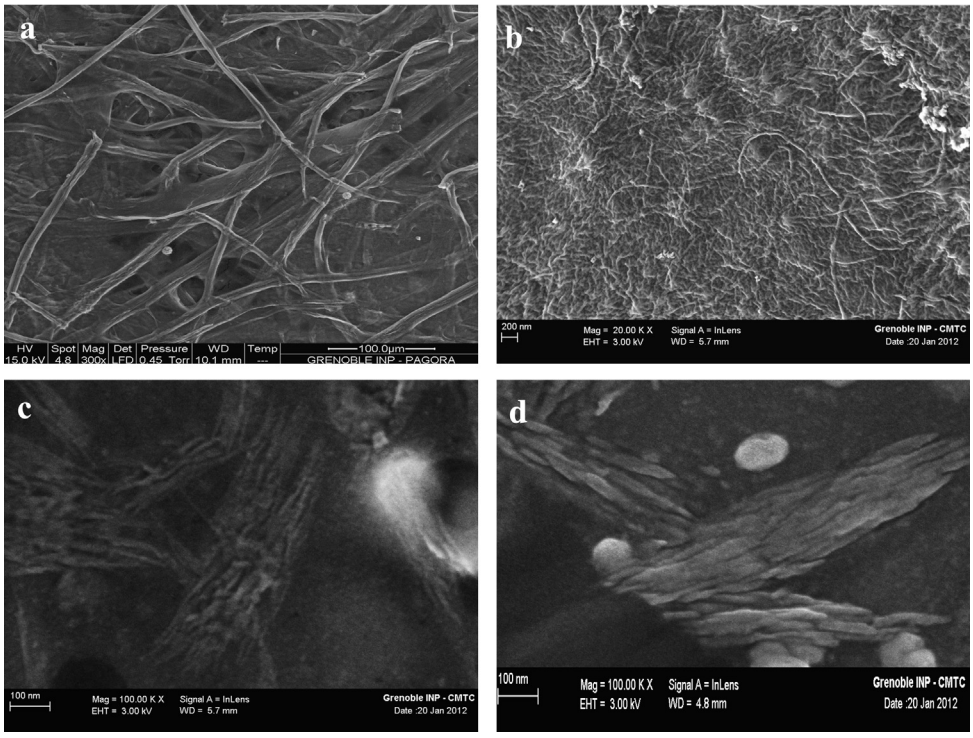

Fig. 3. FE-SEM images of (a) pristine cellulose (sample 1), and NFC obtained after (b) 5 min TEMPO-mediated oxidation (sample 2), (c) 30 min TEMPO-mediated oxidation (sample 4), and (d) 1 h TEMPO-mediated oxidation (sample 5).

duration of the oxidative treatment is increased, the depolymerization through β-elimination of glycoside becomes significant, resulting in shortening of the fibrils and reduction of their aspect ratio (Fig. 3b–d). On the other hand, the width of the fibrils is affected by the oxidation time (or degree of oxidation). Actually, fibrils obtained with higher oxidation times have lower width, i.e. lower than 30 nm (see Fig. 3c and d). This reduction of the fibril width could be explained by the highest ease of NFC release induced by the increase of the degree of oxidation.

X-ray diffraction analyses indicate that the oxidation time does not seem to impact the crystalline structure (see results presented in Table 1). However, the number of passes through the homogenizer seems to reduce the crystallinity index. Actually, the mechanical shearing seems to damage the crystallites through breaking effect or peeling-off mechanism of the cellulose chains (see Table 1). The X-ray diffraction patterns of oxidized NFC are similar to that of the untreated sample (see supporting data S2). This feature also clearly indicates that carboxylic groups are not formed inside cellulose I crystallites during the TEMPO-mediated oxidation, but a significant amount of carboxylate groups formed on fibril surfaces and in disordered regions, in agreement with previous works (Besbes, Rei Vilar, & Boufi, 2011; Montanari et al., 2005; Saito & Isogai, 2004).

Supplementary data related to this article found, in the online version, at http://dx.doi.org/10.1016/j.carbpol.2013.08.032.

4.2. Viscoelastic properties

Dispersions with varying oxidation degrees and concentrations of NFC were subjected to dynamic oscillation strain ramping. The gel properties were described in terms of two dynamic mechanical properties: the elastic modulus G' also known as dynamic rigidity, reflecting the reversibly stored energy of the system, and the viscous modulus G'', reflecting the irreversible energy loss. The results are presented in Figs. 4 and 5. The strain range over which G' is independent of the applied oscillation strain amplitude is called the linear viscoelastic region (LVR), and the end of the linear region is called the critical strain, δ_c. As noted from the graph, the 1 wt% dispersion exhibits significantly higher G' values compared to the 0.6 wt%, 0.4 wt% and 0.1 wt% suspensions as expected. The critical strain δ_c decreases while increasing the NFC concentration indicating the formation of an increasingly stiff network. This phenomenon is due to the increase in the intermolecular interactions between NFC in the dispersion when increasing the concentration. The dispersion with the lowest NFC concentration (0.1 wt%) exhibits G'' values higher than G' values, meaning that at low NFC concentration the viscous properties are dominant compared to the elastic ones and a lower degree of particle association (Henriksson et al., 2007). On the other hand for the 0.1 wt% suspension the linear region covers the whole range of applied oscillation strain amplitude showing that the NFC dispersion displays a liquid behavior regardless the oxidation time (NFC length). However, it is worthy noticing that the gap between G' and G'' decreases and the critical strain δ_c increases when increasing the degree of oxidation. This is directly related to the effect of NFC length reduction. Pääkkö et al. (2007) observed a gel-like behavior for all the NFC suspensions they investigated, even for the lowest concentration as 0.125 wt%. The difference could be explained by the high length of the NFC they studied which were obtained by mild enzymatic pretreatment combined with mechanical shearing. The higher length of NFC enables their earlier percolation via entanglements formation.

Fig. 6 shows the viscoelastic properties of oxidized NFC dispersions as a function of the applied oscillating frequency. It is evident from Fig. 6(a)–(e) that the viscoelastic behavior of the oxidized NFC suspensions changes as function of the NFC concentration. A tendency toward a frequency-dependent profile was clearly observed for 0.1 wt% NFC suspensions for all studied samples. However, a frequency-independent profile is clearly observed when the NFC concentration exceeds 0.4 wt%.

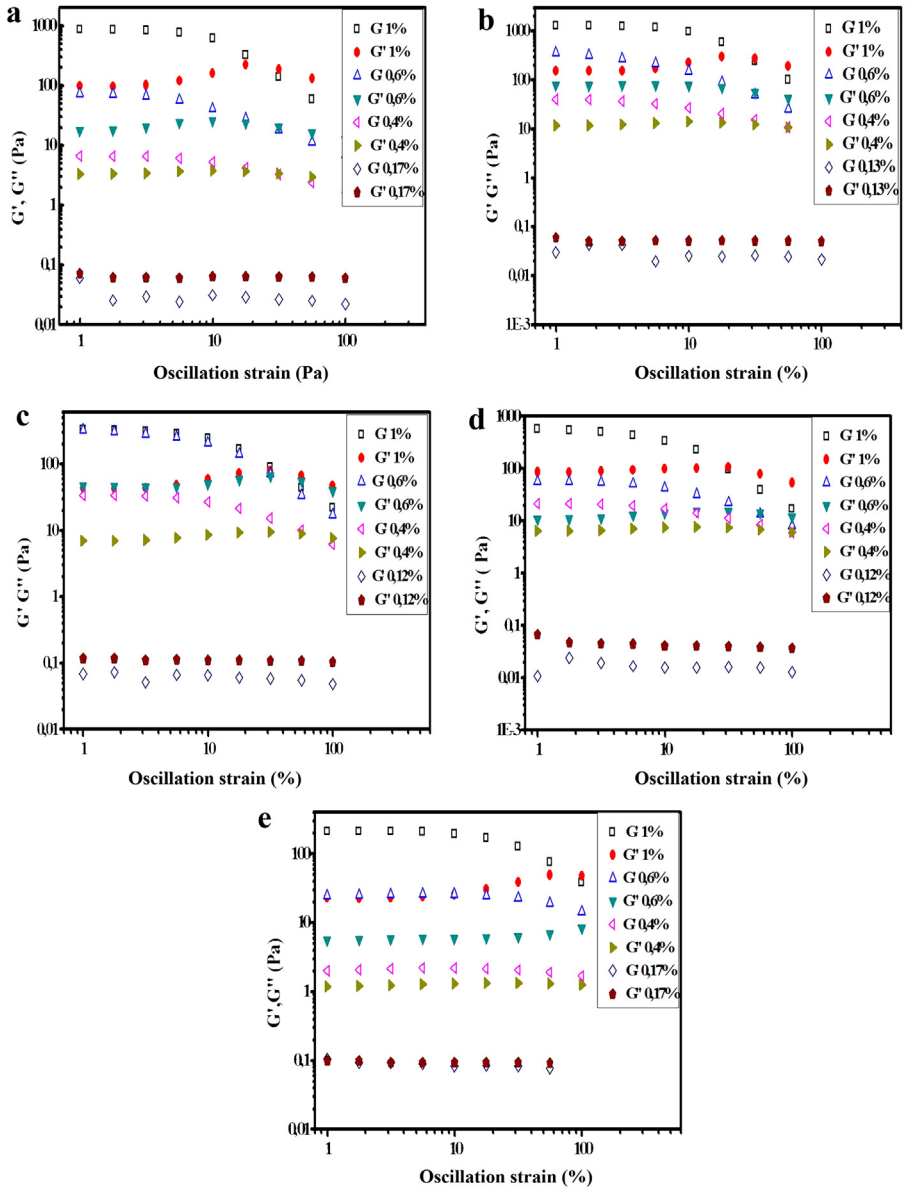

Fig. 4. Storage (G') and loss (G'') modulus vs. oscillation strain for oxidized NFC suspensions at varying concentration: (a) NFC-O-5 min, (b): NFC-O-15 min, (c): NFC-O-30 min, (d):NFC-O-1 h, (e): NFC-O-2 h.

However, the values of the elastic modulus reach 10^3 Pa for the 1 wt% NFC suspensions with low degree of oxidation. These values are high compared to those observed for the same concentration of NFC obtained via enzymatic pretreatment (Pääkkö et al., 2007) even though the NFC we are studying presents relatively lower length. This could be explained by the higher charge of the oxidized NFC surface compared to un-oxidized NFC. These charges develop repulsive forces between NFCS responsible of their good dispersion and at the same time lead to more immobilized water molecules at the vicinity of NFC (bounded water molecules). Then, as far as their degree of oxidation is high their electro-kinetic potential increases and consequently they immobilize more and further away surrounding water molecules. Ono, Shimaya, Sato, and Hongo (2004) used ^{1}H NMR to calculate the amount of immobilized molecules water at the vicinity of NFC. They showed that with increasing ionic strength, the network formation and the successive fibril aggregation occur and both should be interpreted in terms of the electrostatic interaction between negative charge on a cellulose surface and cationic aqueous layer around it.

In addition to the electrokinetic potential of NFC, the fibril entanglements that could develop, particularly for the longest ones, represent another parameter that increases the dispersion modulus. Both parameters seem to be responsible for controlling the stiffness of the suspension. In the present study these two parameters are evolving oppositely. In fact, the increase of the degree of oxidation is accompanied with the reduction of the NFC length and then the probability of entanglement. In addition, and according to FE-SEM observations, the length of NFC with higher degree of oxidation (obtained after 2 h oxidation) is of the same order of magnitude than for cellulose nanocrystals we extracted by acid hydrolysis in our previous work (Bendahou et al., 2009). Even though the value of the elastic modulus reaches only 200 Pa for the concentration of 1 wt% for NFC with higher degree of oxidation, it is high compared to the one observed at the same concentration for cellulose nanocrystals dispersions (Tatsumi, Ishioka, & Matsumoto, 2002). These latter cellulose nanocrystals have an aspect ratio of 42. This comparison shows again the effect of surface charge on the stiffness of the gel.

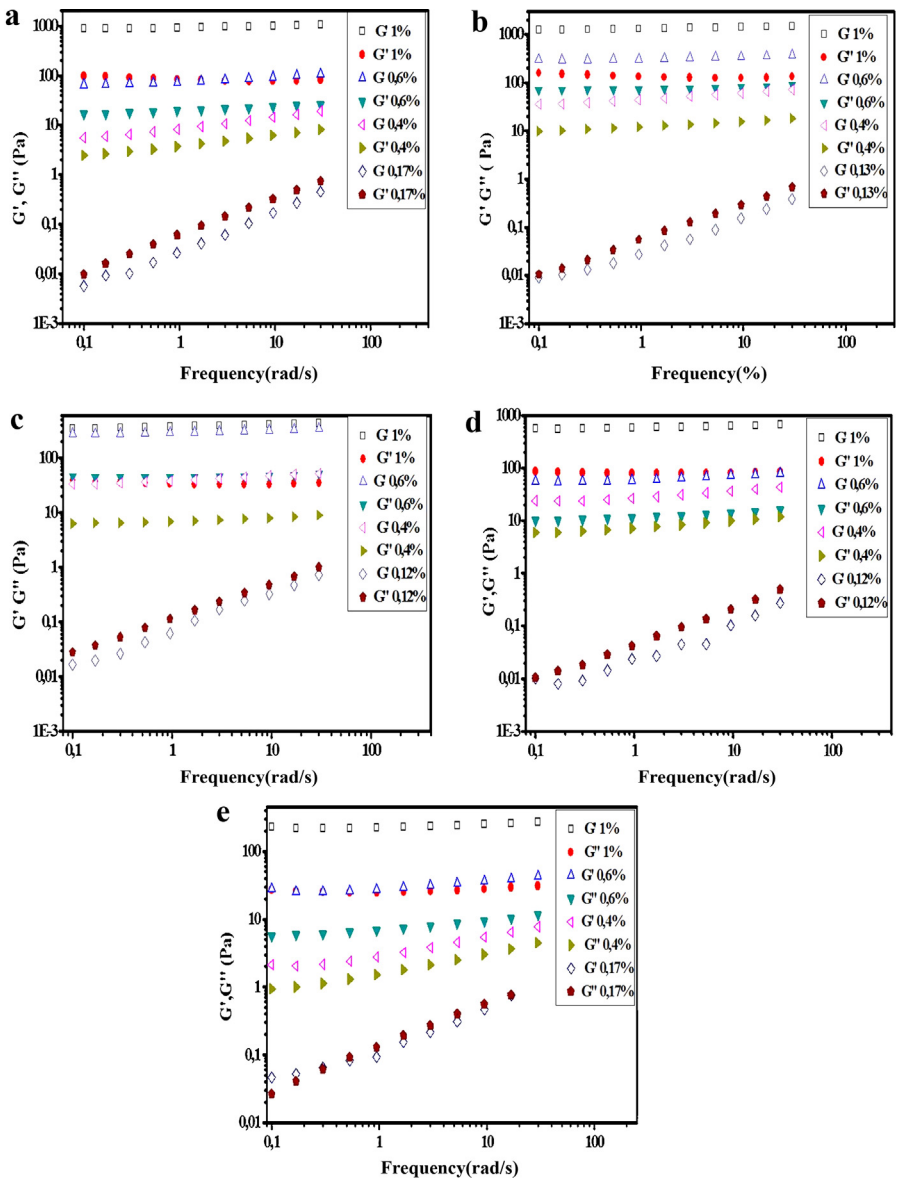

Fig. 5. Storage (G') and loss (G'') modulus vs. frequency for oxidized MFC suspensions at varying concentration: (a) MFC-O-5 min, (b): MFC-O-15 min, (c): MFC-O-30 min, (d): MFC-O-1 h, (e): MFC-O-2 h.

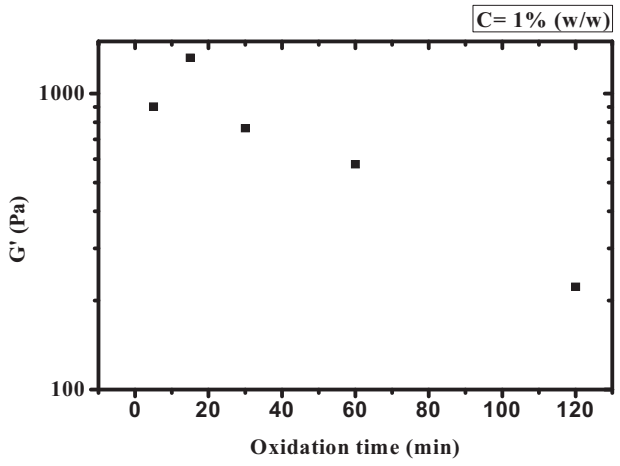

Fig. 6. The elastic modulus G' for 1 wt % oxidized NFC gel samples as a function of oxidation time at the frequency of 1 Hz.

Fig. 6 shows the evolution of the elastic modulus as a function of the oxidation time for the 1 wt% NFC dispersions. It could be clearly seen that the modulus decreases when the oxidation time increases. Even if the increase of NFC surface charge (more immobilization of surrounding water molecules) could not compensate the reduction of the gel stiffness caused by the reduction of the NFC length (reduction of the density of entanglements), it enables to maintain the formation of a stable and relatively strong gel. This is confirmed for all concentrations from 1 to 0.4 wt%. Based on these remarks we propose in Fig. 7a structure model representing the evolution of the gel structure as a function of the oxidation time. By increasing the reaction time the NFC length decreases and their surface charge increases and the gel becomes more dependent on the immobilized water molecules. Because of the repulsive forces between the charges, these later will be positioned at some distance from each other so that they balance (or set aside the effect of) the repulsive force between them. This kind of gel (high oxidation time NFCs based gel) is comparable to the repulsive gels observed, particularly, for clay dispersions that could be obtained in specific ranges of nanoparticles concentrations and ionic strength of the

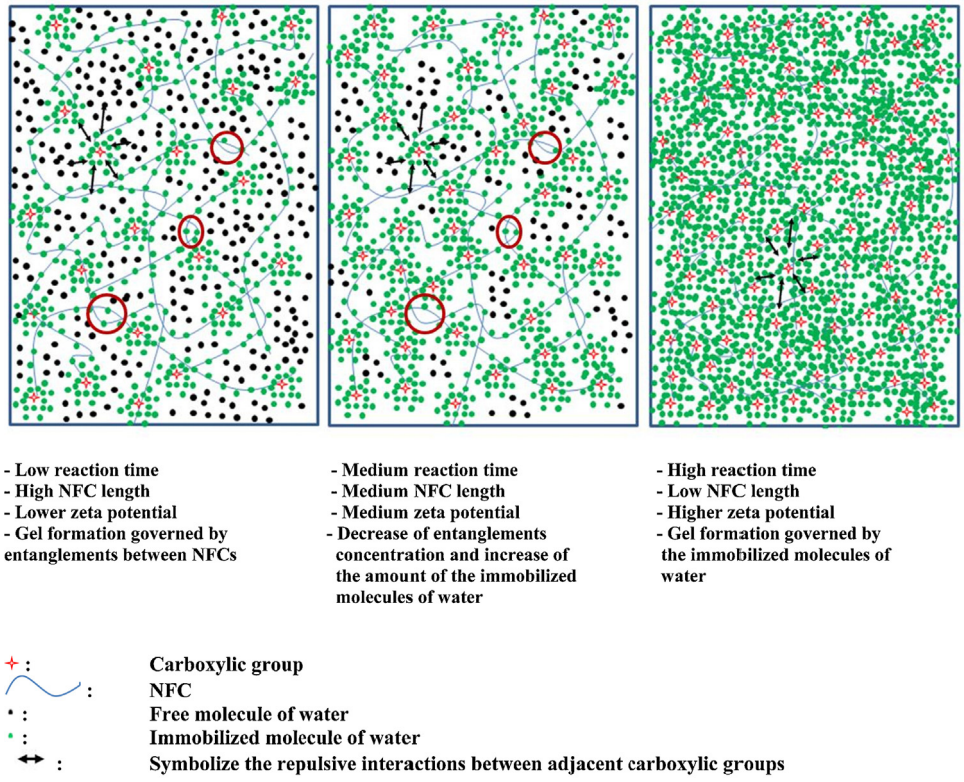

Fig. 7. Gel structure model representing the evolution of the gel structure as function of oxidation time.

medium (Abend & Lagaly, 2000; Benna-Zayani et al., 2009; Tombácz & Szekeres, 2006). The gel properties and the proposed evolution of its nature should be confirmed by additional experiments on the effect of temperature, pH, ionic strength of the medium and concentration. The confrontation of the properties of these gels to the models proposed in literature will bring more clarification of the gel structure.

5. Conclusion

TEMPO-mediated oxidation pretreatment of the rachis of date palm tree under alkaline and low temperature conditions was used to facilitate the extraction of nanofibrillated cellulose (NFC). The effect of experimental parameters such as oxidation time (or degree of oxidation) and the number of passes through the homogenizer on the yield and the geometrical characteristics of the extracted fibrils was investigated using various experimental techniques, such as HPLC, FTIR, conductimetric titration, FE-SEM, DRX, and UV–vis. It was shown that the extraction of NFC from the rachis of date palm tree is relatively easy compared to other plants studied in literature. On the other hand, low oxidation times (or low carboxylic acid contents as 220 μmol/g) are sufficient to extracted high aspect ratio NFC with high yield after three passes through the homogenizer at 650 MPa Increasing the oxidation time facilitates the extraction procedure but degrades the cellulose inducing lowering of the aspect ratio of NFC. We could also show that the number of passes through the homogenizer has a visible effect on the crystallinity index of NFC.

The rheological properties of gels and aqueous dispersions of the prepared NFC were characterized as a function of the oxidation time. Dynamic rheology showed that the behavior changes from liquid to gel depending on the concentration. The higher concentration studied was 1 wt% and the modulus reached 1 MPa which is higher than values reported in literature for gels based non-oxidized NFC. The control of both the NFC aspect ratio and surface charge opens novel applications in materials science, for example, as reinforcement and as filter for cationic adsorption.

Acknowledgement

Hassan II Academy of Sciences and Technologies and PHC VOLUBILIS (grant 24508WD) are gratefully acknowledged for financial support.

References

Abend, S., & Lagaly, G. (2000). Sol–gel transitions of sodium montmorillonite dispersions. *Applied Clay Science*, *16*(3–4), 201–227.
Alila, S., Besbes, I., Rei Vilar, M., Mutjé, P., & Boufi, S. (2013). Non-woody plants as raw materials for production of microfibrillated cellulose (MFC): A comparative study. *Industrial Crops and Products*, *41*, 250–259.
Bendahou, A., Habibi, Y., Kaddami, H., & Dufresne, A. (2009). Physico-chemical characterization of palm from *Phoenix dactylifera* L. preparation of cellulose whiskers and natural rubber-based nanocomposites. *Journal of Biobased Materials and Bioenergy*, *3*, 1–10.
Bendahou, A., Kaddami, H., & Dufresne, A. (2010). Investigation on the effect of cellulosic nanoparticles' morphology on the properties of natural rubber based nanocomposites. *European Polymer Journal*, *46*, 609–620.
Benna-Zayani, M., Mgaidi, A., Stambouli, M., Kbir-Ariguib, N., Trabelsi-Ayadi, M., & Grossiord, J. L. (2009). Fractal nature of bentonite–water–NaCl gel systems evidenced by viscoelastic properties and model of gels. *Applied Clay Science*, *46*(3), 260–264.
Besbes, I., Rei Vilar, M., & Boufi, S. (2011). Nanofibrillated cellulose from alfa, eucalyptus and pine fibres: preparation characteristics and reinforcing potential. *Carbohydrate Polymers*, *84*, 975–983.
Bragd, P. L., van Bekkum, H., & Besmer, A. C. (2004). TEMPO-mediated oxidation of polysaccharides: Survey of Methods and Applications. *Topics in Catalysis*, *27*(1–4), 46–66.
Henriksson, M., Henriksson, G., Berglund, L. A., & Lindstrom, T. (2007). An environmentally friendly method for enzyme-assisted preparation of microfibrillated cellulose (MFC) nanofibers. *European Polymer Journal*, *43*, 3434–3441.
Herrick, F. W., Casebier, R. L., Hamilton, J. K., & Sandberg, K. R. (1983). Microfibrillated cellulose; morphology and accessibility. *Journal of Applied Polymer Science. Applied Polymer Symposium*, *37*, 797–813.
Ishii, D., Saito, T., & Isogai, A. (2011). Viscoelastic evaluation of average length of cellulose nanofibers prepared by TEMPO-mediated oxidation. *Biomacromolecules*, *12*, 548–550.

Montanari, S., Roumani, M., Heux, L., & Vignon, M. R. (2005). Topochemistry of carboxylated cellulose nanocrystals resulting from TEMPO-mediated oxidation. *Macromolecules*, *38*, 1665–1671.

Ono, H., Shimaya, Y., Sato, K., & Hongo, T. (2004). 1H spin–spin relaxation time of water and rheological properties of cellulose nanofiber dispersion. Transparent cellulose hydrogel (TCG). *Polymer Journal*, *36*(9), 684–694.

Pääkkö, M., Ankerfors, M., Kosonen, H., Nykanen, A., Ahola, S., Österberg, M., et al. (2007). Enzymatic hydrolysis combined with mechanical shearing and high-pressure homogenization for nanoscale cellulose fibrils and strong gels. *Biomacromolecules*, *8*, 1934–1941.

Rinaudo, M. (1968). Etude physico-chimique des solutions de cellulose dans le FeTNa. *Papeterie*, *90*, 479–487.

Saito, T., Hirota, M., Tamura, N., Kimura, S., Fukuzumi, H., Heux, L., et al. (2009). Individualization of nanosized plant cellulose fibrils by direct surface carboxylation using TEMPO catalyst under neutral conditions. *Biomacromolecules*, *10*, 1992–1996.

Saito, T., & Isogai, A. (2004). TEMPO-medited oxidation of native cellulose. The effect of oxidation conditions on chemical and crystal structure of the water-insoluble fractions. *Biomacromolecules*, *5*, 1983–1989.

Saito, T., Kimura, S., Nishiyama, Y., & Isogai, A. (2007). Cellulose nanofibers prepared by TEMPO-mediated oxidation of native cellulose. *Biomacromolecules*, *8*, 2485–2491.

Saito, T., Nishiyama, Y., Putaux, J., Vignon, M. R., & Isogai, A. (2006). Homogeneous.suspensions of individualized microfibrils from TEMPO-catalyzed oxidation of native cellulose. *Biomacromolecules*, *7*(6), 1687–1691.

Sbiai, A., Kaddami, H., Sautereau, H., Maazouz, A., & Fleury, E. (2011). TEMPO-mediated oxidation of lignocellulosic fibers from date palm leaves. *Carbohydrate Polymers*, *86*, 1445–1450.

Segal, L., Creely, J. J., Martin, A. E., & Conrad, C. M. (1959). An empirical method for estimating the degree of crystallinity of native cellulose using the X-ray diffractometer. *Textile Research Journal*, *29*, 786–794.

Shibata, I., Yanagisawa, M., Sato, T., & Isogai, A. (2006). SEC-MALLS analysis of cellouronic acid prepared from regenerated cellulose by TEMPO-mediated oxidation. *Cellulose*, *12*, 305–315.

Shinoda, R., Saito, T., Okita, Y., & Isogai, A. (2012). Relationship between length and degree of polymerization of TEMPO-oxidized cellulose nanofibrils. *Biomacromolecules*, *13*, 842–849.

Suh, D. S., Lee, K. S., Chang, P. S., & Kim, K. O. (2007). Physicochemical properties of cellulose selectively oxidized with the 2,2,6,6-tetramethyl-1-piperidinyl oxoammonium ion. *Journal of Food Science*, *72*(5), 235–241.

Turbak, A. F., Snyder, F. W., & Sandberg, K. R. (1983). Microfibrillated cellulose, a new cellulose product: properties, uses and commercial potential. *Journal of Applied Polymer Science: Applied Polymer Symposium*, *37*, 815–827.

Tatsumi, D., Ishioka, S., & Matsumoto, T. (2002). Effect of fiber concentration and axial ratio on the rheological properties of cellulose fiber suspensions. *Journal of Society of Rheology, Japan*, *30*(32), 27–32.

Tombácz, E., & Szekeres, M. (2006). Surface charge heterogeneity of kaolinite in aqueous suspension in comparison with montmorillonite. *Applied Clay Science*, *34*(1–4), 105–124.